Available online at www.sciencedirect.com
SCIENCE DIRECT®
Journal of Nuclear Materials 323 (2003) 346–353
journal of nuclear materials
www.elsevier.com/locate/jnucmat

Accumulation of point defects and their complexes in irradiated metals as studied by the use of positron annihilation spectroscopy – a brief review

M. Eldrup *, B.N. Singh

Department of Materials Research, Risø National Laboratory, DK-4000 Roskilde, Denmark

Abstract

During the last few years positron annihilation spectroscopy (PAS) has gained increasing recognition as a useful tool in studies of the accumulation of point defects and their complexes in irradiated metals. The technique is sensitive to both the size (in the range from monovacancies up to cavities containing 50–100 vacancies) and the density of vacancy clusters. In order to illustrate the potential of the PAS technique, we present a brief review of results obtained in our laboratory. One series of data show the distinct difference in microstructure between neutron irradiated bcc iron and fcc copper as a function of both irradiation and post-irradiation annealing temperature. Another set of results show the presence of sub-nanometre voids whose size and density increase with dose in neutron irradiated iron. The results show that PAS can be an important experimental tool for the validation of modelling of radiation produced microstructures.

PACS: 61.80.−x; 61.80.Hg; 78.70.Bj; 71.60.+z

1. Introduction

In the vast number of studies carried out of the effects of radiation on the microstructure of materials, the electron microscopy techniques have been the major experimental methods to obtain information about the accumulation of point defects and their complexes. Several other techniques also contribute to the understanding of details of the radiation damage processes. One of these that has gained increasing recognition during the last few years is positron annihilation spectroscopy (PAS). One major advantage of PAS in studies of point defects and their complexes is its sensitivity to the size of vacancy clusters in the range from monovacancies up to cavities big enough to be resolved by TEM.

At Risø National Laboratory, PAS has been used for studies of defects and their clusters for a number of years. In a previous publication [1] we discussed the potentials of PAS by showing results obtained for various metals (aluminium, copper and iron) irradiated with different types of particles, such as electrons, protons, neutrons and helium.

In the present contribution, after a brief introduction to PAS (Section 2), we shall review some recent results obtained in our laboratory on neutron irradiated copper and iron. The results highlight the difference between the microstructures of the two metals, and they illustrate the ability of PAS to produce size distributions of voids too small to be observed by TEM.

2. Brief introduction to positron annihilation spectroscopy

The physical basis for the use of positrons in defect studies is the fact that positrons injected into a material may get trapped at defects that represent regions where the atomic density is lower than the average density in

* Corresponding author. Tel.: +45-4677 5728; fax: +45-4677 5758.
E-mail address: morten.eldrup@risoe.dk (M. Eldrup).

0022-3115/$ - see front matter © 2003 Elsevier B.V. All rights reserved.
doi:10.1016/j.jnucmat.2003.08.011

the bulk, i.e., vacancies, vacancy clusters (including voids, bubbles and SFTs) and dislocations. Since positrons and electrons are antiparticles, an injected positron will annihilate with an electron of the material. As a result, gamma rays will be emitted. These γ-quanta carry information about the state of the positron before annihilation, and by proper measurement of the emitted γ-quanta, it is therefore possible to obtain useful information about those defects that have trapped the positrons.

Normally, regions of lower-than-average atomic density also have lower-than-average electron density. The lifetime of positrons trapped in defects will depend on the average electron density in the defects (the lower the electron density, the longer is the lifetime). So in principle, each type of defect gives rise to a characteristic positron lifetime, τ_i, and by measuring these lifetimes, information is obtained about the defects. This is in brief the physics behind the so-called positron annihilation lifetime spectroscopy (pals). Pals is just one of several different PASs. A more detailed discussion of PAS can be found in e.g., [1,2] and references therein. In the present paper only results obtained by the positron lifetime technique will be reviewed to illustrate the potential of PAS.

A measurement with the positron lifetime technique provides the distribution of lifetimes of the positrons injected into the specimen, the so-called positron lifetime spectrum. Fig. 1 shows examples of positron lifetime spectra for neutron irradiated Cu and Fe. In particular for the spectra for Fe it is clear that some of the spectra are composed of more than one component, which signals the presence of one or more types of defects. Each component is a decaying exponential, the slope of which equals the annihilation rate ($= \tau_i^{-1}$).

Lifetimes of positrons in metals are typically in the range from ~100 to ~500 ps. In bulk Fe and Cu the positron lifetimes are 106 and 110 ps, respectively, while in defects such as monovacancies, dislocations, loops and SFTs the lifetimes are found to be in the range of ~120 to ~180 ps [4–11]. The lifetime of positrons trapped in three-dimensional vacancy agglomerates (voids) increases with void size up to a saturation value of about 500 ps for voids containing more than ~40–50 vacancies [1,8–10]. Thus, for small, sub-microscopic voids (that we shall refer to as 'nano-voids') the lifetime value is a measure of their size.

Trapping of positrons into one type of defects takes place in competition with trapping into other types of defects and with annihilation in the bulk. This competition has been modelled by simple rate equations, often referred to as the 'trapping model' [1]. If the trapping rates are comparable to the annihilation rate of the positrons in the bulk, the trapping model can be used to obtain quantitative estimates of these trapping rates. Trapping rates can normally to a good approximation

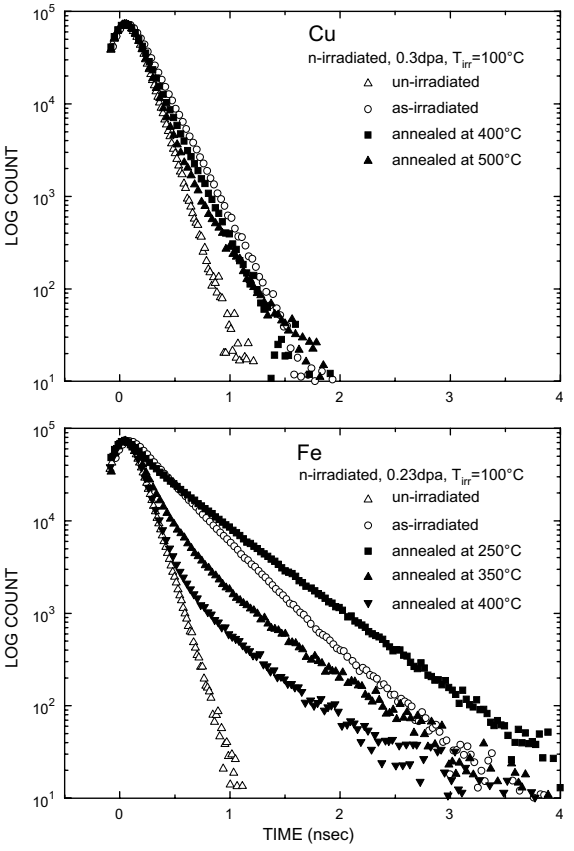

Fig. 1. Examples of PAS lifetime spectra for irradiated and annealed pure copper (top) and pure iron (bottom) [3]. The spectra for Fe clearly contain components with much longer lifetimes than the spectra for Cu. Such long lifetimes are indicative of the presence of three-dimensional vacancy clusters ('nano-voids').

be assumed to be proportional to the concentrations of the defects, i.e.,

$$\kappa_i = \mu_i \times C_i, \tag{1}$$

where κ_i is the trapping rate into the defects of type 'i' and C_i their density. Hence, if the so-called specific trapping rate μ_i is known, the defect densities can be estimated. The specific trapping rate is different for different types of defects. Theoretical estimates have been made of μ_i for various defect types and compared with values determined experimentally [12]. For voids, for example, the experimental estimate of μ_{void} demonstrates that it increases with void size [1].

3. Applications to defect studies

In a previous publication [1] we discussed the positron annihilation technique, exemplified by results of

studies of electron irradiated molybdenum, void formation in neutron, proton and electron irradiated copper, helium bubble formation in aluminium and the annealing behaviour of helium bubbles in copper. In the present communication we shall briefly review some examples of results for neutron irradiated iron and copper, based on measurements primarily carried out in our laboratory. These results comprise comparisons of (1) neutron irradiated Fe and Cu as a function of irradiation temperature and (2) as a function of annealing temperature, as well as (3) the damage evolution in Fe with increasing irradiation dose.

3.1. Neutron irradiated Fe and Cu; influence of irradiation temperature

Fig. 2 shows the positron lifetimes and intensities for Cu and Fe neutron irradiated at different temperatures. There is a clear difference in the results presented for the two metals. Up to 200 °C the longest lifetime in Cu is constant, $\tau_2 = 180 \pm 3$ ps. This lifetime has been associated with small vacancy clusters [3,4,7,11] but may also arise from positrons trapped at truncated SFTs (see below). At 250 and 350 °C, also a third component with a longer lifetime τ_3 of about 500 ps appears. This latter lifetime component is the evidence for the presence of voids [10]. In contrast, the results for Fe show a $\tau_3 \sim 500$ ps at all irradiation temperatures. In addition, at 50 and 100 °C a lifetime τ_2 of about 320 ps gives evidence for the presence of small three-dimensional vacancy agglomerates (nano-voids, containing ~10 vacancies [9]). At 200 and 350 °C τ_2 reduces to 180–200 ps and its intensity I_2 also decreases, while the intensity I_3 of the void component shows a maximum at about 200 °C. Thus, in Cu voids can only be detected for irradiation temperatures close to and above stage V, while in Fe voids are seen in the whole temperature range, including nano-voids at the lower temperatures, with the average void size being bigger at the higher irradiation temperatures.

A plausible explanation for the observed differences between the copper and iron results is considered to arise from the differences in the intracascade clustering of self-interstitial atoms (SIAs) and vacancies and properties of these clusters in fcc Cu and bcc iron. At temperatures well below stage V the production of sessile SIA clusters and SFTs in Cu leads rapidly to a high density of thermally stable clusters, preventing a build-up of a vacancy supersaturation necessary for efficient

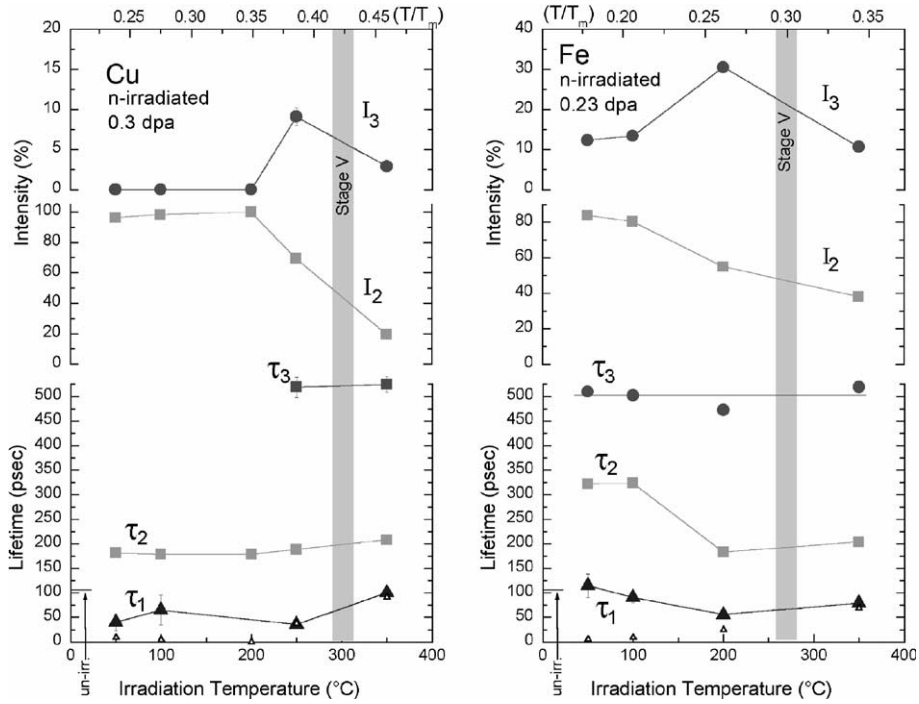

Fig. 2. Positron lifetimes and intensities for neutron irradiated Cu and Fe as functions of irradiation temperature [13,14]. The shaded bands indicate the centers of the recovery stage V in the two metals. For all irradiation temperatures in Fe and for high temperatures in Cu a lifetime of $\tau_3 \sim 500$ ps signals the presence of voids; in Fe at low temperatures an intense ($I_2 \sim 80\%$) component with a lifetime of $\tau_2 \sim 325$ ps shows the presence of a high density of nano-voids, while in Cu the lifetime $\tau_2 \sim 180$ ps is associated with small vacancy clusters or non-perfect SFTs.

void nucleation. It is only for temperatures at and above stage V that vacancies begin to evaporate from the sinks (e.g., SFT, vacancy loops etc.) causing an overall decrease in the sink density and an increase in vacancy supersaturation, thus providing the necessary driving force for void nucleation and growth. In contrast, in bcc iron practically all SIA clusters produced in the cascades are glissile [15] and no SFT are produced. This means that a large fraction of vacancies produced in cascades escape recombination with self-interstitials, which leads to a high local vacancy supersaturation. Thus, already at temperatures above stage III, a high supersaturation of vacancies and hence a high density of voids would result.

The trapping model [1,16] can be used to estimate the trapping rate, κ_2 and κ_3, for positron trapping into nano-voids and voids, respectively, in Fe. The variations of these trapping rates with irradiation temperature are shown in Fig. 3. The strong decrease of the trapping rates with increasing irradiation temperature reflects a decrease of nano-void and void densities. Quantitative estimates of the densities may be obtained by using Eq. (1). At the lower temperatures, κ_2 for Fe is $\geqslant \sim 100$ ns^{-1}. The specific trapping rate for nano-voids containing about 10 vacancies is $\mu \sim 8 \times 10^{15}$ s^{-1} [1]. This leads to a lower limit for the nano-void density of $\sim 1 \times 10^{24}$ m^{-3} ($\sim$13 ppm), which seems to be a reasonable estimate since a similar density of visible voids has been observed by TEM in Mo neutron irradiated under similar conditions [17]. The density of voids cannot be estimated from the PAS data alone, since the saturation lifetime of $\sim$500 ps gives no information about the void size (hence the specific trapping rate cannot be deduced). However, using TEM data for the void sizes, densities determined by PAS are found to be in good agreement with those from TEM [18,19].

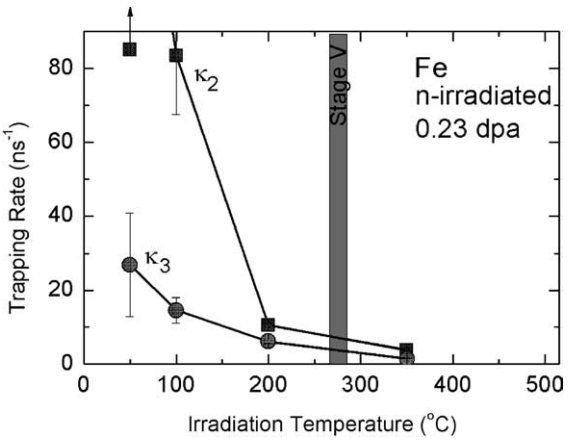

Fig. 3. Positron trapping rates into defects in the neutron irradiated Fe as functions of irradiation temperature, derived from the data for Fe in Fig. 2. The circles are for trapping into voids ($\tau_3 \sim 500$ ps) and the squares into nano-voids (at 50 and 100 °C) or small clusters (at higher temperatures). The strong decrease of the trapping rates with increasing irradiation temperature reflects a decrease of nano-void and void densities. The shaded band indicates the temperature of the recovery stage V [13].

3.2. Neutron irradiated Fe and Cu; influence of post-irradiation annealing temperature

As mentioned above, Fig. 2 shows a clear difference in the defect populations between as-irradiated Cu and Fe. Experimental results demonstrate that the annealing behaviour too is very different for the two metals after neutron irradiation at low temperatures (50 or 100 °C) as shown qualitatively by the changes in the measured lifetime spectra in Fig. 1. The results of the quantitative analysis of the data are shown for Fe and Cu in Fig. 4 (lifetimes and intensities) [3,13] and in Fig. 5 (trapping rates).

As seen in Fig. 4 the longest lifetime for Cu stays constant ($\tau_2 \sim$180 ps) up to about 400 °C while its intensity remains constant (almost 100%) up to $\sim$250 °C but decreases at higher temperatures. This decrease is reflected in the rapid decrease of the trapping rate (Fig. 5), which shows that the density of defects detected by the positrons drops rapidly above $\sim$250 °C. The nature of this defect has been under some debate [3]. The lifetime of $\sim$180 ps suggests a defect of the size of a mono- or di-vacancy. However, the dominant defect population observed in TEM consists of a high density (~ 1–4×10^{23} m^{-3}) of SFTs (of sizes in the range 2–5 nm) [20,21], and perfect SFTs of these sizes are expected to give rise to positron lifetimes of about 130 ps or lower [6,11,22]. If there are defects other than SFTs that give rise to the $\sim$180 ps component, their density must be appreciably higher than the SFT density to dominate the positron trapping. Another possibility could be that a major fraction of the SFTs are not perfect, but have defects associated with them, for example in the form of truncation. A change of this fraction during annealing would show up in the PAS results. This possibility will be further discussed in [21]. At 450 °C and above, the longest lifetime τ_2 increases to about 350 ps, which is characteristic for small three-dimensional vacancy agglomerates, i.e., cavities such as nano-voids ($\sim$10–15 vacancies) or gas bubbles [8].

In the results for Fe, on the other hand, the presence of the two lifetime components with lifetime values of $\tau_2 \sim 325$–375 ps and $\tau_3 \sim 500$ ps demonstrates the existence of nano-voids and voids in the as-irradiated state as well as at the lowest annealing temperatures. The lifetime, $\tau_2 \sim 325$–375 ps, is equivalent to average cavity sizes of $\sim$9–14 vacancies [9]. The longer lifetime of $\sim$500 ps must be associated with voids that contain (on average) $\sim$40–50 vacancies or more. Fig. 4 shows that the

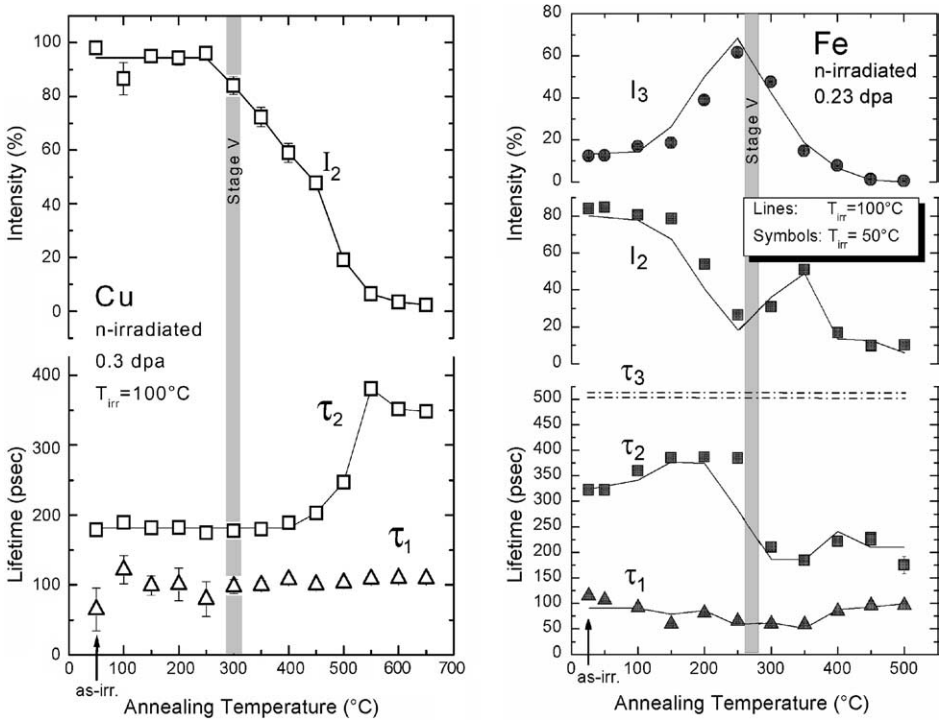

Fig. 4. Positron lifetimes and intensities extracted from the lifetime spectra for neutron irradiated Cu and Fe as functions of annealing temperature. Annealing was done in vacuum and the holding time at each temperature was 50 min. Measurements were carried out at room temperature. Some of the spectra are shown in Fig. 1. For Cu only two lifetime components can be resolved, while for Fe three components can be extracted. For iron, the symbols are for irradiation at 50 °C while the lines represent results for irradiation at 100 °C [13]. For copper, irradiations were carried out at 100 °C [3]. The shaded bands indicate the temperature of the recovery stage V in the two metals.

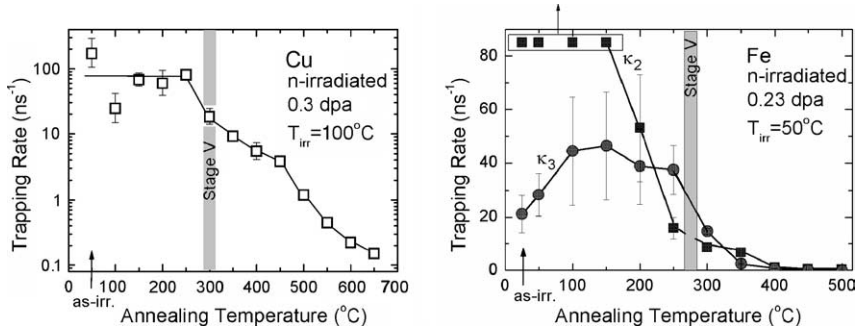

Fig. 5. Positron trapping rates into defects in neutron irradiated Cu and Fe as functions of annealing temperature. The trapping rates, calculated from the data in Fig. 4 by using the 'trapping model', are measures of defect densities [3,13].

annealing behaviour of the PAS parameters for the iron specimens irradiated at 50 °C and at 100 °C is very similar. As a consequence, also the variation of the trapping rates with annealing temperature is very similar (Fig. 5 and [3]). The changes of the PAS parameters in different temperature ranges reflect the recovery of the microstructure during annealing. The following are the main observations.

In the annealing temperature range of 50 °C to about 250 °C, κ_3 first increases and then flattens off (Fig. 5) which suggests that the density and/or the size of the voids increases and then stays constant. Simultaneously,

κ_2 and therefore the nano-void density decreases drastically while the increase of τ_2 (up to 250 °C, Fig. 4) indicates an increase in the average nano-void size from less than 10–15 vacancies. Thus, the number density of voids increases at the expense of the nano-voids. This strong coarsening of the nano-void population takes place at temperatures well below the recovery stage V (250–280 °C [23]) the centre of which is indicated by a grey band in Figs. 4 and 5. Since stage V indicates the lower temperature at which vacancies can evaporate from nano-voids or voids, the decrease in density of the nano-voids below stage V must happen by their migration and coalescence with other nano-voids and voids [24,25].

When the annealing temperature increases above stage V, τ_2 drops abruptly (Fig. 4). This indicates that the nano-void component disappears in this temperature range, which is also indicated by the steep decrease of κ_2 that extrapolates to zero at about Stage V (Fig. 5). Above Stage V, $\tau_2 \approx 200$ ps, which is a lifetime that could be due to gas or impurity stabilised vacancy clusters containing only a few vacancies, as mentioned earlier. Their density may be estimated to be $\sim 5\times 10^{23}$ m^{-3} [3] up to about 350 °C. Above 350 °C the density decreases to the detection limit at ~500 °C.

In the temperature range 250–350 °C, i.e., in and above the annealing stage V, the trapping rate for voids κ_3 decreases by a factor of more than ten (Fig. 5) and continues to decrease at the higher temperatures. This demonstrates clearly that in stage V the void density decreases, probably by coarsening of the void population due to Ostwald ripening.

An interesting result for the irradiated iron is that there is no significant difference between the PAS results for irradiation at 50 °C and at 100 °C (Fig. 4) neither for the as-irradiated nor the annealed specimens. This is contrary to the electrical conductivity results, which show a clear difference between the data for iron irradiated at 50 °C and at 100 °C [13,26]. This difference may be associated with trapping of defects by impurity carbon atoms below the migration temperature for carbon (>70 °C).

3.3. Dose dependence of defect accumulation in neutron irradiated iron

As discussed above, nano-voids were observed in iron that was neutron irradiated at about room temperature to a dose of 0.23 dpa. In relation to this, it was interesting to investigate at which dose voids might begin to nucleate and how the void population in Fe might evolve as a function of dose during irradiation at low temperatures. Results of such an investigation for displacement damage doses in the range of 10^{-4} to 0.23 dpa [26] are briefly discussed below.

In the results for iron discussed in the previous sections, two defect components were resolved from the measured positron lifetime spectra and the two lifetimes were associated with specific average void sizes. However, such an analysis should be considered as a two-bin representation of a wide size distribution of cavities rather than a measure of the presence of only two discrete cavity sizes.

In order to try to determine a multibin size distribution, the lifetime spectra for Fe were analysed on the assumption that they were composed of five components, four of which have fixed lifetimes: 200, 300, 400 and 500 ps, equivalent to three-dimensional vacancy clusters of sizes of about 0.35, 0.54, 0.73 and >1.0 nm in diameter, respectively. From the intensities of these lifetime components and by using the 'trapping model' combined with Eq. (1) (Section 2 and [1]), the defect densities C_i for the different cavity sizes were estimated [26].

The size distributions obtained this way for the three-dimensional vacancy clusters in Fe are shown in Fig. 6 for different doses. The size (for a cluster of N_v vacancies) is given by an equivalent diameter, i.e., the diameter of a sphere with a volume equal to N_v vacancies. Clearly, it has been possible to derive an estimate of the cavity size distribution for different doses. With increasing

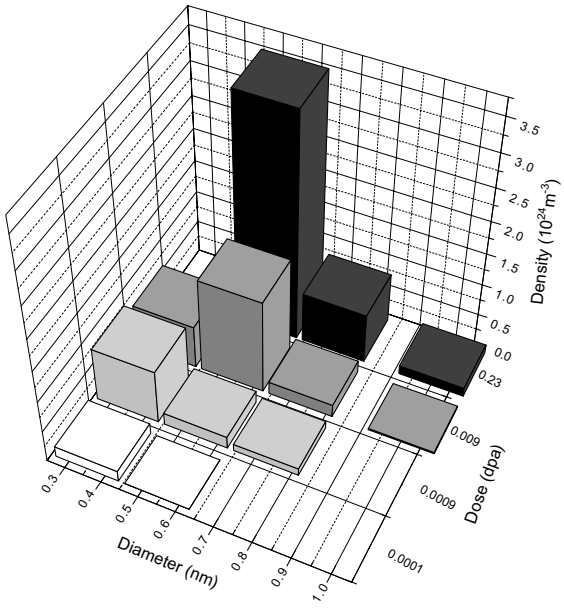

Fig. 6. Size distributions for three-dimensional vacancy clusters in Fe that was neutron irradiated to different doses (T_{irr} = 50–70 °C). The distributions were derived from PAS data as briefly explained in the text. The size (for a cluster of N_v vacancies) is given by an equivalent diameter, i.e., the diameter of a sphere with a volume equal to N_v vacancies [26].

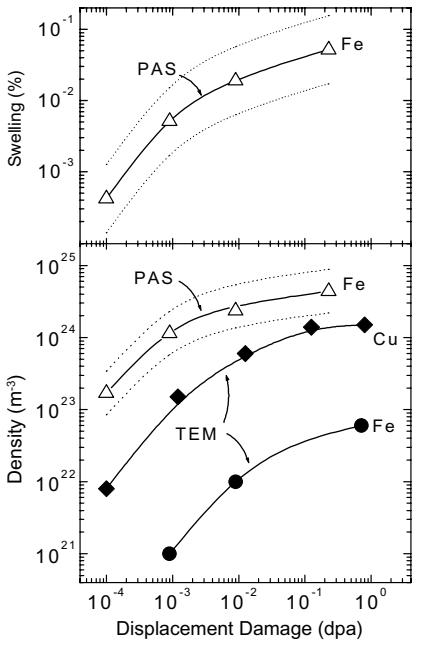

Fig. 7. Dose dependence of defect cluster density in neutron irradiated Fe. For comparison the density of SFTs in Cu is also shown (◆). In Fe the TEM results (●) are mainly densities of interstitial clusters, while the PAS results (△) are the total density of three-dimensional vacancy clusters obtained from Fig. 6. At the top of the figure, the dose dependence of the swelling derived from the PAS data for Fe is shown. The dotted curves indicate estimated uncertainty bands for both density and swelling [26].

dose, both the density and the average size increase. The total density of the three-dimensional vacancy clusters as a function of dose is shown in Fig. 7. The calculated swelling, S, is also plotted in Fig. 7. For doses lower than ~0.01 dpa, the swelling increases roughly linearly with dose, with a swelling rate of $\sim 4 \pm 2\%$/dpa. At higher dose the swelling levels off. The presence of small cavities was confirmed by TEM for specimens irradiated to a dose of 0.7 dpa [26]. Soneda et al. [27] have carried out kinetic Monte Carlo simulations of the microstructure evolution in neutron irradiated Fe. It is interesting that the result of their simulation is apparently in good agreement with the experimental data shown in Fig. 7.

4. Conclusions

The present note demonstrates that PAS can provide valuable quantitative information about the microstructure of irradiated metals, not least about the behaviour of voids and sub-microscopic voids (nanovoids). This makes PAS a potentially important experimental tool for the validation of results of modelling of radiation produced microstructures.

The series of investigations reviewed above have firmly established that in bcc iron void nucleation occurs already at temperatures just above the recovery stage III, whereas in fcc copper void nucleation does not occur until the irradiation temperature is close to or above stage V.

Acknowledgement

The present work was partly funded by the European Fusion Technology Programme.

References

[1] M. Eldrup, B.N. Singh, J. Nucl. Mater. 251 (1997) 132.
[2] M. Eldrup, J. Phys. (Paris) IV Colloq. 5 (1995) C1.
[3] M. Eldrup, B.N. Singh, J. Nucl. Mater. 276 (2000) 269.
[4] M. Eldrup, J.H. Evans, O.E. Mogensen, B.N. Singh, Radiat. Eff. 54 (1981) 65.
[5] Y. Kamimura, T. Tsutsumi, E. Kuramoto, Phys. Rev. B 52 (1995) 879.
[6] E. Kuramoto, H. Abe, M. Takenaka, F. Hori, Y. Kamimura, M. Kimura, K. Ueno, J. Nucl. Mater. 239 (1996) 54.
[7] K. Ueno, M. Ohmura, M. Kimura, Y. Kamimura, M. Takenaka, T. Tsutsumi, K. Ohsawa, H. Abe, E. Kuramoto, Mater. Sci. Forum 255–257 (1997) 430.
[8] K.O. Jensen, R.M. Nieminen, Phys. Rev. B 36 (1987) 8219.
[9] M. Puska, R.M. Nieminen, J. Phys. F: Metal Phys. 13 (1983) 333.
[10] M. Eldrup, Mater. Sci. Forum 105–110 (1992) 229.
[11] H. Häkkinen, S. Mäkinen, M. Manninen, Phys. Rev. B 41 (1990) 12441.
[12] M. Puska, R.M. Nieminen, Rev. Mod. Phys. 66 (1994) 841.
[13] M. Eldrup, B.N. Singh, Risø-R-1241 (EN), Risø National Laboratory, 2001, p. 21.
[14] M. Eldrup, B.N. Singh, Mater. Sci. Forum 363–365 (2001) 79.
[15] Yu.N. Osetsky, A. Serrra, B.N. Singh, S.I. Golubov, Philos. Mag. A 80 (2000) 2131.
[16] R.N. West, Adv. Phys. 22 (1973) 263.
[17] S.I. Golubov, B.N. Singh, H. Trinkaus, J. Nucl. Mater. 276 (2000) 78.
[18] B.N. Singh, M. Eldrup, A. Horsewell, P. Ehrhart, F. Dworschak, Philos. Mag. A 80 (2000) 2629.
[19] B.N. Singh, M. Eldrup, S.J. Zinkle, S.I. Golubov, Philos. Mag. A 82 (2002) 1137.
[20] B.N. Singh, D.J. Edwards, P. Toft, J. Nucl. Mater. 299 (2001) 205.
[21] D.J. Edwards et al., unpublished.
[22] E. Kuramoto, T. Tsutsumi, K. Ueno, M. Ohmura, M. Kimura, Y. Kamimura, Computat. Mater. Sci. 14 (1999) 28.
[23] H. Schultz, P. Ehrhart, in: H. Ullmaier (Ed.), Landolt-Börnstein New Series, vol. 25, Springer, Berlin.
[24] P.J. Goodhew, S.K. Tyler, Proc. R. Soc. A 377 (1981) 151.

[25] B.N. Singh, A.J.E. Foreman, in: R.S. Nelson (Ed.), Consultant Symposium; The Physics of Irradiation Produced Voids, AERE-R7934, H.M. Stationary Office, January 1975, p. 205; Scr. Mater. 9 (1975) 1135.
[26] M. Eldrup, B.N. Singh, S.J. Zinkle, T.S. Byun, K. Farrell, J. Nucl. Mater. 307–311 (2002) 912.
[27] N. Soneda, S. Ishino, A. Takahashi, K. Dohi, these Proceedings.